Moving Obstacle Avoidance in Indoor Environments

Ahmad Alsaab, Robert Bicker

Abstract— This paper deals with a problem of autonomous mobile robot navigation among dynamic obstacles. The velocity obstacle approach (VO) is considered an easy and simple method to detect the collision situation between two circular-shaped objects using the collision cone principle. The VO approach has two challenges when applied in indoor environments. The first challenge is that in the real world, not all obstacles have circular shapes. The second challenge is that the mobile robot cannot sometimes move to its goal because all its velocities to the goal are located within collision cones. For indoor environments some unobserved moving objects may appear suddenly in the robot path; particularly when the robot crosses a corridor or passes an open door. The contributions of this paper are that a method has been proposed to extract the collision cones of non-circular objects, where the obstacle size and the collision time are considered to weigh the velocities of the robot, and the virtual obstacle principle has been proposed to avoid unobserved moving objects. The experiments were conducted within indoor environments to validate the control algorithm proposed in this paper, and results obtained showed the mobile robot successfully avoided both static and dynamic obstacles.

Index Terms— Collision cone, Dynamic obstacle, Indoor navigations, Mobile robot, Non-circular object, Unobserved obstacles, Velocity obstacle approach.

1 INTRODUCTION

Autonomous ability of mobile robots provides large application areas including routine tasks such as office cleaning and delivery, access to dangerous areas that are unreachable by humans such as cleanup of hazardous waste sites in nuclear power stations and planetary explorations. The key challenge of a mobile robot is to avoid obstacles which may prevent it from reaching its goal. Many algorithms have been suggested to solve this problem such as the potential field algorithm (PFA) and the vector field histogram method (VFH), however these methods do not consider the kinematic constraints of the mobile robot such as limited velocities and accelerations [1], [2]. The Dynamic Window Approach (DWA) considers these constraints, where a suitable pair of rotation and linear speeds is chosen to avoid obstacles through a circular path, but it needs relatively long time to define the free collision velocities [3]. All the previous mentioned algorithms are suitable for avoiding static obstacles. The linear velocity obstacle algorithm (VO) was proposed to avoid moving obstacles, where it defines the collision situation between two circular objects moving with constant velocities [4]. The non-linear V-Obstacle method was introduced as an extension of the VO algorithm to avoid obstacles moving on arbitrary trajectories [5].

The first challenge of the VO algorithm is that in the real workspace, not all obstacles have circular shapes. The second challenge is that the mobile robot cannot sometimes move to its goal because all its velocities to the goal are located within collision cones as shown in Fig.1 , but there is at least one safe path to the goal. Many studies have been implemented the VO algorithm using simulation, furthermore they considered that obstacles have circle shapes and their velocities are known. For instance, [6] , [7] proposed the probabilistic collision cone principle, where the grown obstacle is extended by uncertainty in the exact radii of the obstacle and robot, the collision probability in the exact collision cone is given a value 1, while into the uncertain area the collision probability is given a value between 1 and 0 . However, they have not considered the collision time. In [8], [9], the grown obstacle radius was modified depending on the collision distance and collision time. This algorithm can be applied to avoid circular obstacles. For non-circular obstacles, the robot has to fit the sensor data into circles using a circle fitting method [10], [11], [12]. The optimal time horizon principle has been proposed in [13], where the smallest time horizon is used to define the collision course velocities. In the simulation test, they used circular obstacle and considered the obstacle's speed known, however in the real world the robot has to extract the shapes of the obstacle from sensor data, grow them using the robot radius and then extract the collision cones.

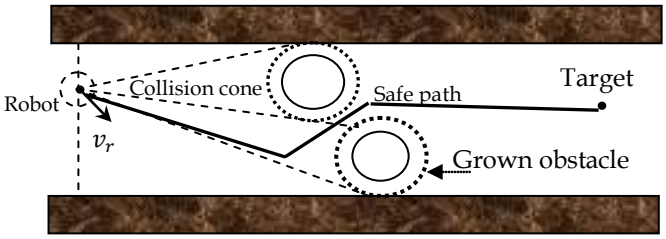

Fig. 1. The robot cannot reach its target according to the VO method

A mobile robot avoids dynamic obstacles by collecting information about its surrounding environment using sensors. It then clusters the sensor data and utilizes a tracking algorithm to estimate the velocities and locations of obstacles. 2D scanning laser sensors are common in mobile robot applications, provide accurate information about the robot workspace, require a relatively small computation time and are unaffected by changes in illumination.

There are two types of laser data cluster methods; the distance-based clustering methods [14], [15], [16] and kalman filter-based methods [17]. The KF-based methods detect the segments and their directions precisely, but are more complex than the distance-based methods and require relatively large computa-

tion time.

Some unobserved moving objects may appear suddenly in the robot's path; particularly when the robot crosses a corridor or passes an open door. The robot must be able to anticipate such scenarios and manoeuvre to avoid collisions. The mobile robot can define the opened doors and corridors by extracting walls from the sensor data. There are many methods to extract walls from the laser data such as the Hough Transform Algorithm, line regression method, line tracking algorithm and iterative-end-point-fit algorithm [18], [19,] [20], [21], [22]. This paper uses the Iterative-end-point-fit algorithm which is considered as a simple and robust method to extract lines from 2D laser sensors.

In this work, reactive control architecture was adopted, where a 2D laser sensor was utilized to recognize the robot's workspace and the laser data was clustered using the distance-based clustering method proposed in [16]. The extended particle filter algorithm (EXPF) proposed in [23] was used to estimate the obstacle velocity. A method was demonstrated to extract the collision cones of circular and non-circular objects. Furthermore, the collision time and the obstacle size were considered. The virtual obstacle principle was proposed to avoid unobserved obstacles which may appear from opened doors.

2 Reactive Control System

Reactive control architecture was adopted in this study to produce the control command for the mobile robot as shown in Fig. 2, the sensor data comes from the laser sensor and odometry data. In the first stage, the laser data is clustered into separate groups (obstacles) using the distance-based clustering method proposed in [16]. In the second stage, the obstacles velocities are estimated by a tracking algorithm using the extended particle filter. While the third stage includes three behaviours namely Go to Goal, Obstacle Avoidance and Unobserved obstacle avoidance. In the fourth stage, the outputs of the behaviours are fused to produce the control commands.

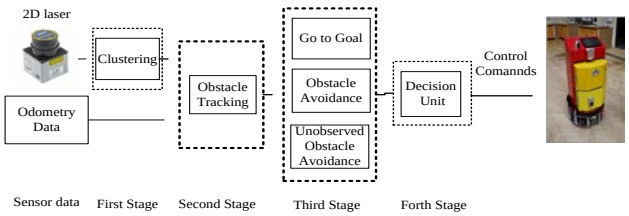

Fig. 2. The proposed reactive control system

2.1 Go to Goal Behaviour

This behaviour utilizes the current robot position coming from the odometry sensors and the goal position to define the speed and direction to the target. In the global reference frame, the angle to and the distance between the robot and the target are given as:

$$\theta_t = \tan^{-1}(y_t - y_r, x_t - x_r) \quad (1)$$

$$d_t = \sqrt{(x_t - x_r)^2 + (y_t - y_r)^2} \quad (2)$$

where (x_t, y_t) and (x_r, y_r) represent the target and robot positions with respect to the global reference frame. d_t represents the distance between the robot and the target.

The reference speed to the target is given as following:

$$v_t = \begin{cases} v_{max} & if\ d_t > d_{th} \\ v_{max}\dfrac{d_t}{d_{th}} & otherwise \end{cases} \quad (3)$$

where v_{max} and d_{th}denote the robot's maximum speed and threshold distance respectively.

2.2 Obstacle Avoidance behaviour

2.2.1 Collision Cone of non-circular Obstacle

The original velocity obstacle method supposes that the robot and obstacle have circular shapes. The boundary of collision cone is defined by the two tangents of the grown obstacle circle and the centre of the robot as shown in Fig. 3. The left and right angles of the tangents are given as following:

$$d = \sqrt{(x_o - x_r)^2 + (y_o - y_r)^2} \quad (4)$$

$$L = \sqrt{d^2 - r^2} \quad (5)$$

$$\emptyset = \tan^{-1}((y_o - y_r)/(x_o - x_r)) \quad (6)$$

$$\emptyset_l = tan^{-1}(\frac{r}{L}) + \emptyset \quad (7)$$

$$\emptyset_r = -\tan^{-1}\left(\frac{r}{L}\right) + \emptyset \quad (8)$$

where d is the distance between the robot centre and the obstacle centre, L is the tangent length, $\emptyset$ is the angle between the obstacle and the robot in the global frame, $\emptyset_l, \emptyset_r$ are the left and right tangent angles, $(x_r, y_r), (x_o, y_o)$ are the robot and obstacle coordination.

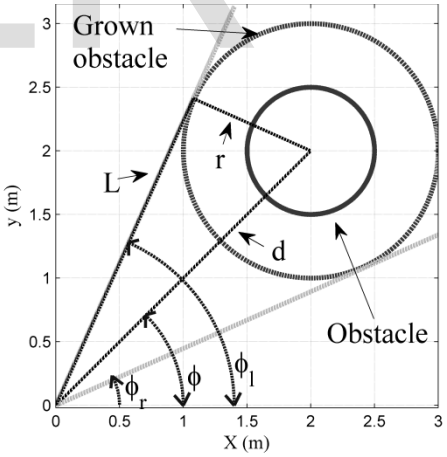

Fig. 3. Velocity obstacle approach

Suppose there is a circular obstacle as shown Fig. 4, in which some points in the obstacle circumference were grown by the robot radius r_r. It can be noticed that the outer boundaries of the grown points produced the grown obstacle circle. However, the left and right tangent angles θ_{li}, θ_{ri} of a grown point can be calculated using equations [4],[5],[6], [7], [8]. The collision cone boundaries of the obstacle are determined by the right tangent which has the minimum angle and the left tangent which has the maximum angle.

In this project a method is proposed to find the actual collision cone of a non-circular obstacle by the following steps:

- Each laser point is grown by robot radius.

- Calculating the left tangent angles θ_{l1} ,,, θ_{ln} and right tangent angles θ_{r1} ,,, θ_{rn} of the grown laser points, where n refers to total number of laser points.
- Taking the maximum of the left tangent angles θ_{l1} ,,, θ_{ln} represents the left tangent angle of the grown obstacle, and the minimum value of the right tangent angles θ_{r1} ,,, θ_{rn} represent the right tangent angle

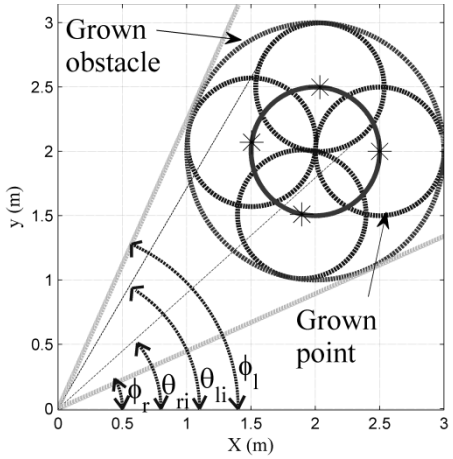

Fig. 4. Growing the circumference points

2.2.2 Considering the collision time and obstacle size

The collision time and obstacle size are considered by assigning the robot velocities with different weights. Thus all free collision velocities are given weights of numeric value 1, while the weights of the collision course velocities are given as follows:

$$Ws_i = \begin{cases} 0 & if\ t_c(i) < t_{cth} \\ \exp\left(\frac{-a}{t_c(i)}\right) * \left(1 - b * \delta * t_c(i)\right) & otherwise \end{cases} \quad (9)$$

$$\delta = \min(\emptyset_l - \theta_i, \theta_i - \emptyset_r) \quad (10)$$

where $t_c(i)$ refers to the collision time. a, b are constants, t_{cth} is the critical collision time, θ_i is the velocity angle.

The robot velocities within a collision cone have different collision distances depending on the obstacle shape. However the collision distance of the robot velocity (v_i, θ_i) is given as:

$$d_c(i) = laserdata(I) \quad (11)$$

$$I = floor(\theta_i/\sigma) \quad (12)$$

where $laserdata, I$ and σ refer to return laser points, index and the angle resolution of the laser sensor respectively. $floor$ is a function which gives the integral value.

2.3 Unobserved Obstacle Avoidance

In indoor environments, some unobserved moving objects may appear suddenly in the robot path; particularly when the robot crosses a corridor or passes an open door. Therefore the robot has to consider these obstacles and implement an action to minimize the collision risk with the unobserved obstacles.

In this project a simple method was introduced to meet this requirement. The virtual obstacle principle has been proposed to avoid unobserved moving objects, in which a virtual circular obstacle is created at the start point of each open door threshold and corridor cross as shown in Fig. 5. The virtual radius is modified depending on the robot speed as the following equation:

$$r_o = R.v_i \quad (13)$$

where R is a constant positive value. v_i represents the robot speed

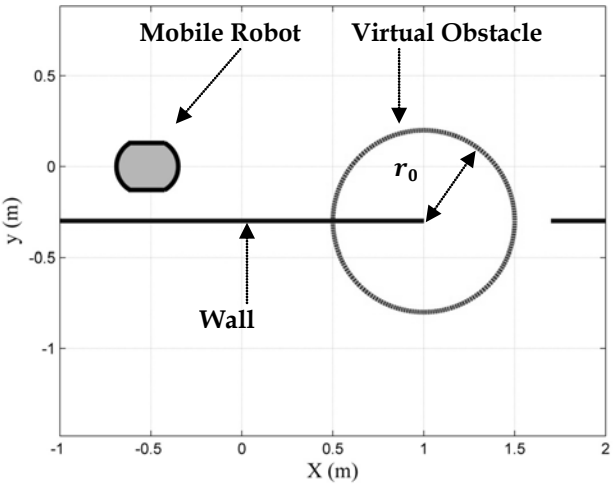

Fig. 5. The Virtual obstacle principle

The collision cone of the virtual obstacle is calculated depending on the equations [3],[4],[5],[6], [7]. Likewise In this behaviour, the robot velocities are weighed according the following:

$$W_{unob} = \begin{cases} 1 & if\ d_{ro} > d_{th} \\ \exp\left(-\frac{a_{unob}}{t_c(i)}\right) * \left(1 - b_{unob} * \delta * t_c(i)\right) \end{cases} \quad (14)$$

a_{unob} , $b_{unob}$and d_{th} are constants. d_{ro} refers to the distance between the robot and the door threshold.

2.4 Decision unit

The main task of this block is to fuse the outputs of the behaviours and then generate the control commands which minimize the collision risk and maximize the speed to the goal. The robot velocities are weighted depending on the output of the Go to Goal behaviour and the weights coming from the Obstacle Avoidance and Unobserved avoidance behaviours.

$$w_i = \min(W_{unob}, \mathrm{Ws}) * (\alpha_1 + \cos(\theta_t - \theta_i)) * (\alpha_2 - \|v_t - v_i\|) \quad (15)$$

where α_1, α_2 are constants.

The maximum weight velocity (v_c, θ_c) is chosen to produce control commands given as:

- The rotation speed is given as:

$$\omega_c = k_w.\theta_c \quad (16)$$

where k_w is constant

- The linear speed is given as

$$V_c = \begin{cases} v_c & if\ v_c < V_{cmax} \\ 0 & if\ 0 > V_{cmax} \\ V_{cmax} & otherwise \end{cases} \quad (17)$$

$$V_{cmax} = v_{max} - k_v . \frac{\omega_c}{\omega_{max}} \quad (18)$$

where k_v is a constant, v_{max} and ω_{max} represent the maximum linear and rotation speeds of the mobile robot.

3 RESULTS AND DECISION

Experiments were implemented using two robots; the Pioneer P3-DX robot and Nubot robot which was made in Newcastle University. The experiments aimed to show that the robot can avoid collision with obstacles which have different intelligence levels, and minimize the collision risk with unobserved moving objects. Obstacles were classified according to the obstacle avoidance method into three classes; non-intelligent obstacles which do not have any obstacle avoidance algorithm, the low-level intelligent obstacles have ability to avoid static obstacle, and intelligent obstacles (Human).

The maximum linear and rotation speeds of the robots were adjusted to 0.5 m/s and 100 degree/s respectively. In equation [3], the threshold distance was chosen to be d_{th} = 1 m. The parameters of the weighting fuction in equations [9], [14] for the obstacle avoidance and unobserved obstacle avoidance behaviours were chosen to be a = a_{unob}=5, b = b_{unob} = 0.5. The constant value in equation [13] was chosen tobe 0.5m.the parameters a_1 and a_2 in equation [15] were assigned to the values 0.1 and 0.6 respectively. The parameters k_w and k_v were selected to be 1 and respectively.

3.1 Collision Cone

The collision cone produced by the method demonstrated in this paper is compared with that produced by two fitting circle algorithms proposed in [11], [12]. Fig. 6 shows a virtual non-circular obstacle, in which the laser angle resolution was chosen to be 5°. The returned laser points are listed in Table 1.

TABLE 1
COLLECTED LASER POINTS

Laser point	1	2	3	4
Angle(degree)	40	45	50	55
distance	1.4	1	1.14	1.8

Fig. 7 shows the fitted circles; the circle C1 is produced by applying the method proposed in [11], while the circle C2 is produced by the method proposed [12]. Obviously the circle C1 is relatively huge which produces a huge collision cone. Therefore the comparison was made between the collision cones produced by the circle C2 and the algorithm developed in this study.

The calculated radius of the circle C2 was 0.36m which was grown by the robot radius0.5m. As result the calculated angle of the collision cone of the circle C2 was 70°. However it can be seen from Fig. 8 that the collision cone does not touch any point of the grown laser points.

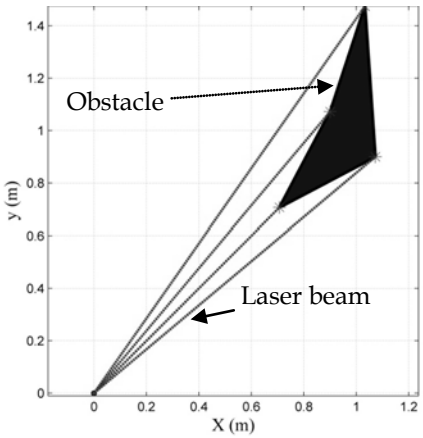

Fig. 6. Non-circular obstacle

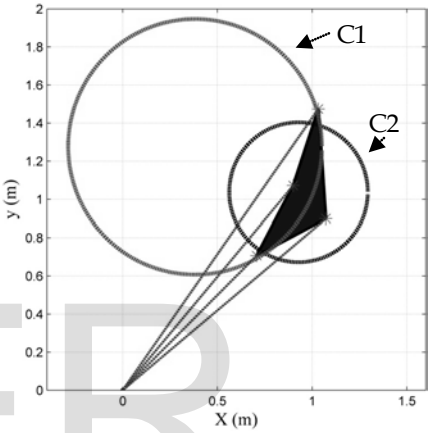

Fig. 7. Fitted obstacle circles

For the proposed method, Table 2 lists the calculated tangent angles of each grown laser point, it can be noticed that the second point has the maximum left angle and minimum right angle. Hence, it is not always correct to find the collision cone based on the first and last laser points of the laser cluster. The angle of the collision cone produced by the proposed method is 60°. Fig. 9 shows that the collision cone touches the grown obstacle at two points. Clearly the proposed method produced a collision cone which is more accurate and smaller than that produced by the circle fitting methods.

TABLE 2
COLLISION CONES FOR THE GROWN LASER POINTS

Laser point	1	2	3	4
Left angle(degree)	60.1	75	70.1	71.1
Right angle (degree)	19	15	29	38.8

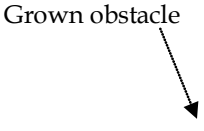

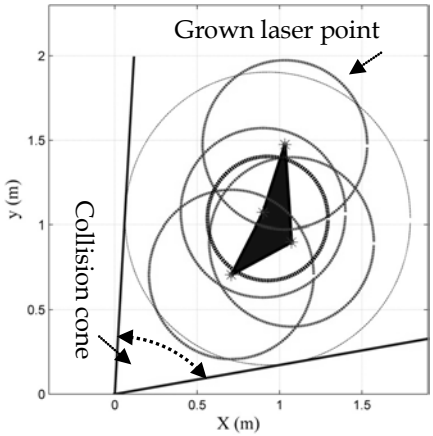

Fig. 8. Collision cone of the fitting circle

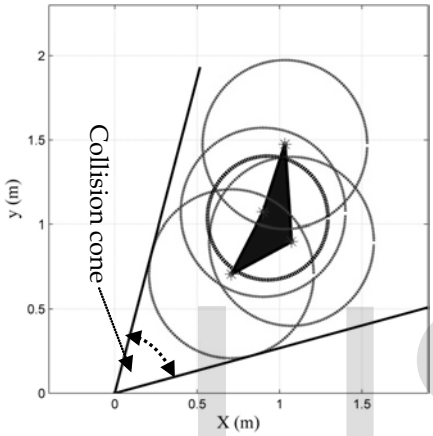

Fig. 9. Collision cone of the proposed method

3.2 Passing through a narrow Gap

The mobile robot (Pioneer P3-DX) had to pass through a narrow gap as shown in Fig. 10. The robot's start point and target were chosen to be ($x_r = 0m, y_r = 0m$) and ($x_t = 3m, x_t = 0m$) respectively, while the narrow gap was located at $x = 1.55$ m. The widths of the robot and narrow space were 0.45 m and 0.6 m respectively. Therefore the robot had free spaces of 75 mm at each side whilst passing through the narrow gap.

Fig. 10. The mobile robot has to pass the narrow gap

Fig. 11 shows that the robot was able to pass the narrow space without any collision. It can be seen that the robot implemented approximately a straight line during passing the narrow space and then it turned to the goal in a curved path. On hand Fig. 12 shows the robot speed vs. the x coordinate of the mobile robot, in which the robot speed was increased form 0 m/s at $x = 0$ m to achieve the maximum speed of 0.5 m/s at$x = 0.6$ m. When the robot became close to the gap at $x = 1.42$ m it started to decrease, the speed became 0.34 m/s at $x = 1.57$ m and then it increased after passing the narrow gap. When the robot became close to its goal the speed was decreased gradually to become0 m/s.

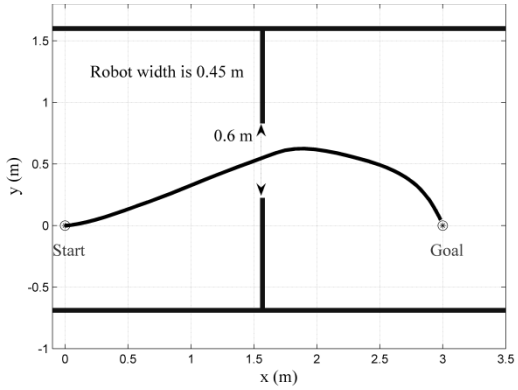

Fig. 11. The mobile robot was able to pass the narrow gap

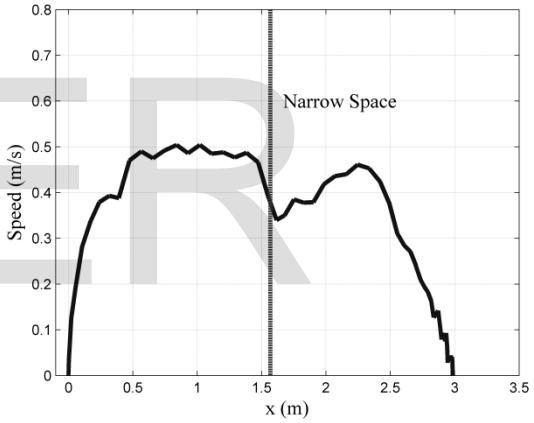

Fig. 12. The mobile robot speed

3.3 Avoiding a non-intelligent obstacle

The intelligent mobile robot (Pioneer robot) had to avoid a non-intelligent obstacle (Nubot Robot) Fig.13. The Nubot robot was not given any avoidance collision algorithm and moved with a fixed speed0.5 m/s. The start positions of the robot and obstacle were chosen as ($x_r = 0m, y_r = 0m$) and ($x_t = 5m, x_t = 0m$) respectively. Fig.14. shows that The Pioneer robot was able to avoid the non-intelligent obstacle without any collision. It can be seen that the Pioneer robot moved on a straight line from $t = 0s$ till $t= 3.6$ s , and then avoided the moving obstacle, while at $t = 7.5$ s after the moving obstacle passed the robot turned to its goal.

3.4 Avoiding a low-level intelligent moving obstacle

Here the Nubot robot having the ability to avoid static obstacles based on the potential field algorithm, where it used the laser data to produce the repulsive forces and the odometry data to produce the attractive force. The Pioneer started to avoid the Nubot robot at $t = 3$ s as shown in Fig. 15. After the dynam-

ic obstacle passed the mobile robot turned to its goal (5m, 0 m) at the moment t = 8 s. On other side the low-level intelligent Nubot robot implemented a small avoidance manoeuvre thereby avoiding the Pioneer robot at the momentt = 7 s. Clearly the Pioneer robot started the avoidance manoeuvre 4 s before the Nubot robot.

Fig. 13. The Nubot robot and Pioneer robot

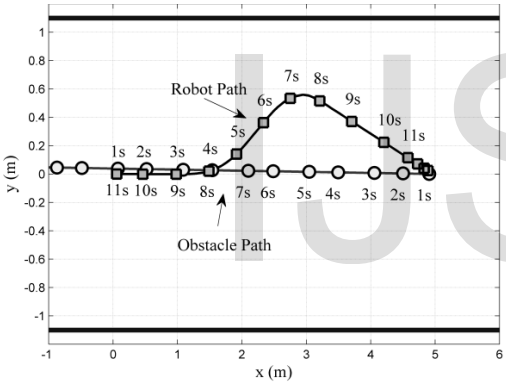

Fig. 14. The robot avoided a non-intelligent obstacle

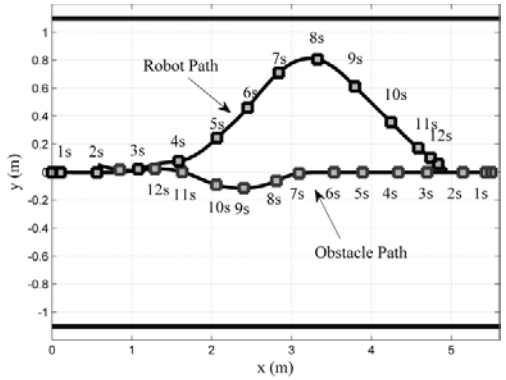

Fig. 15. The robot avoided a low-intelligent obstacle

3.5 Avoiding an intelligent moving obstacle

In this test, the robot had to avoid a human. As shown in Fig. 16 the robot turned to its right side at the moment t=3.74s to avoid human, but also the human turned to the same direction at the moment t=4s. Thus the robot turned right to avoid collision with human. The estimated of the human was 0.85 m/s.

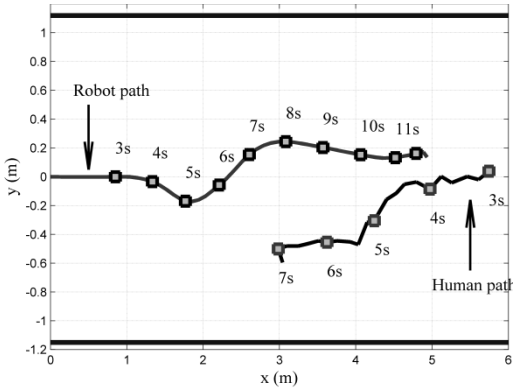

Fig. 16. The robot avoided a human

3.4 Avoiding two dynamic obstacles

In this test, the robot had to avoid an obstacle moving in the same direction (Nubot) and an obstacle moving in the opposite direction (Human). The speed of the Nubot robot was adjusted as 0.35 m/s. As shown in Fig. 17, the human appeared in the laser data at the moment t=4s and disappeared at t=7s. On other side, the robot changed its direction to follow the moving obstacle (Nubot) and avoid the human at the moment t=4.8s, and after the human passed, the robot started to avoid the obstacle and reach its goal.

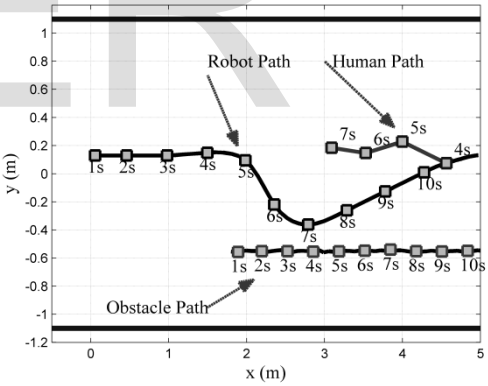

Fig. 17. The robot avoided an obstacle and human

4.5 Unobserved obstacle avoidance

The experiment workspace is shown in Fig. 18, in which the robot was located close to the wall. The robot had to reach its goal ($x = 6.5m, y = -3.3m$) without causing colliding with any obstacle. To avoid any causing damage to the robots, a simulation test using Player/Stage simulator was carried out to show that the robot may collide with an unobserved obstacle if it does not use the virtual obstacle principle. Fig. 19 shows the mobile robot collided with obstacle because the unobserved obstacle avoidance was removed from its control system.

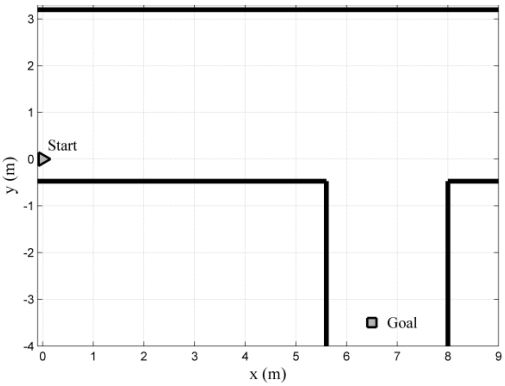

Fig. 18. The robot has to go to the goal and avoid an unobserved obstacle

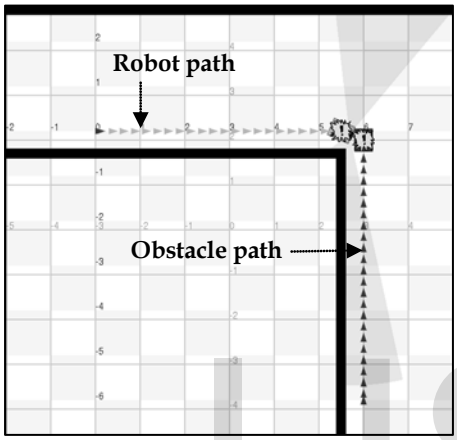

Fig. 19. The mobile robot collided with the unobserved (simulation test)

Two real experiments were implemented for avoiding unobserved obstacles, Fig. 20 shows that the robot started to go away from the corner at the moment t=12s, while the dynamic obstacle appeared in the laser data at the moment t=17s, at the moment t=18s the robot turned right to maximum the speed to its goal, but at the moment t=20s, the robot turned left again to avoid the collision with the dynamic obstacle. After the dynamic obstacle passed the robot returned to its goal.

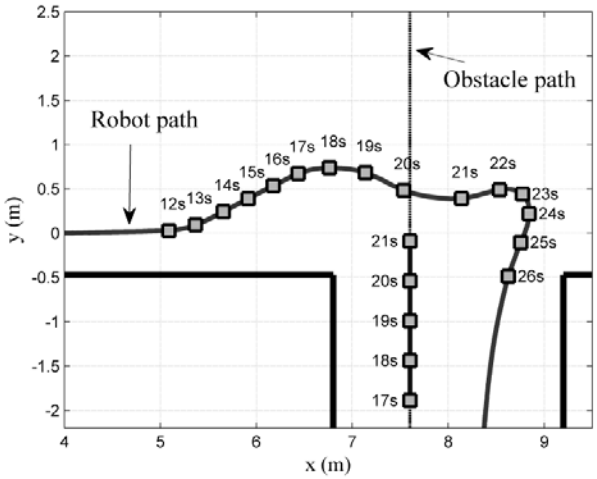

Fig. 20. The mobile robot (Poineer) avoided the unobserved dynamic obstacle (Nubot)

In second test, the obstacle appeared in the laser data at the moment t=15s as shown in Fig. 21. At the moment t=17s the robot reduced it speed and turned right to allow the moving obstacle to pass without any collision, after the collision risk with moving obstacle disappeared at the moment t=21s the robot started to increase it speed and turn to its goal.

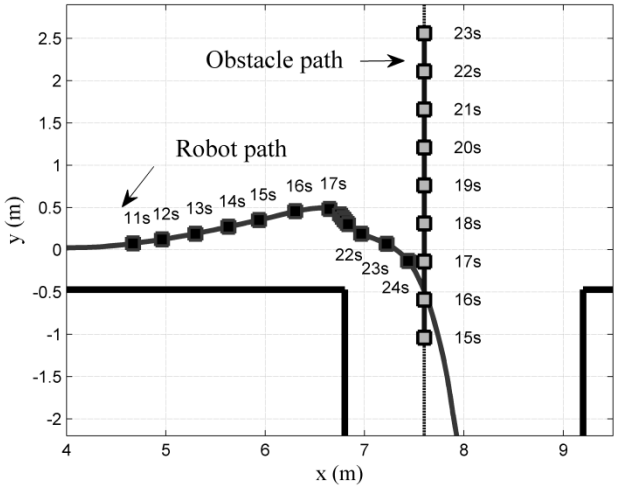

Fig. 21. The mobile robot (Pioneer) waited the unobserved dynamic obstacle (Nubot) to pass

4 Conclusion

In this paper, reactive control architecture has been adopted for mobile robot navigation in indoor environments. A simple method has been proposed to find the collision cones of circular and non-circular obstacles using a laser sensor, in which each laser point was grown by the robot radius, where the maximum left tangent represented the left boundary of the collision cone of the grown obstacle, and the minimum right tangent represented the right boundary of the collision cone. The result has showed that the collision cone produced by the proposed method is more accurate and smaller if compared with that produced by the circle fitting methods. The collision time and the obstacle size were also considered to weigh the robot velocities.

The virtual obstacle principle has been proposed to avoid unobserved moving objects may appear suddenly form open doors, where a virtual circular obstacle is created at the start point of each door or corridor cross. The simulation test showed that the robot collided with an unobserved obstacle because the unobserved obstacle avoidance behaviour was removed from the control system, while the experiments showed that the robot was able to avoid unobserved obstacle appearing from corridor cross when the robot used the unobserved obstacle behaviour. Finally almost of the experiments have been captured and posted in the following website:
https://www.facebook.com/pages/Robotics-Group/173949736063997

References

[1] O. Khatib, "Real-time obstacle avoidance for manipulators and mobile robots," in in Robotics and Automation. Proceedings. 1985 IEEE International Conference, 1985, pp. 500–505.

[2] J. Borenstein and Y. Koren, "The vector field histogram-fast obstacle avoidance for mobile robots," in Robotics and Automation, IEEE Transactions on, vol. 7, 1991, pp. 278–288.

[3] D. Fox, W. Burgard, and S. Thrun, "The dynamic window approach to collision avoidance," in Robotics and Automation Magazine, IEEE, vol. 4, 1997, pp. 23–33.

[4] P. Fiorini and Z. Shiller, "Motion planning in dynamic environments using velocity obstacles," in International Journal of Robotics Research, vol. 7, 1998, pp. 760–772.

[5] Large, Frederic, Laugier, Christian, and Z. Shiller, "Navigation among moving obstacles using the nlvo: Principles and applications to intelligent vehicles," in Autonomous Robots, vol. 19, 2005, pp. 159–171.

[6] B. Kluge, "Recursive agent modeling with probabilistic velocity obstacles for mobile robot navigation among humans," in in Intelligent Robots and Systems, 2003. (IROS 2003). Proceedings. 2003 IEEE/RSJ International Conference on, vol. 1, 2003, pp. 376–380.

[7] B. Kluge and E. Prassler, "Reflective navigation: individual behaviors and group behaviors," in in Robotics and Automation, 2004. Proceedings. ICRA '04. 2004 IEEE International Conference on, vol. 4, 2004, pp. 4172–4177.

[8] Z. Xunyu, P. Xiafu, and Z. Jiehua, "Dynamic collision avoidance of mobile robot based on velocity obstacles," in in Transportation, Mechanical, and Electrical Engineering (TMEE), 2011 International Conference on, 2011, pp. 2410–2413.

[9] M. Yamamoto, M. Shimada, and A. Mohr, "Online navigation of mobile robot under the existence of dynamically moving multiple obstacles," in in Assembly and Task Planning, 2001,

[10] [J. Guivant, E. Nebot, and H. Durrant-Whyte, "Simultaneous localization and map building using natural features in outdoor environments," in Intelligent Autonomous Systems VI, 2000, pp. 581–588.

[11] W. Gander, G. H. Golub, and R. Strebel, "Least squares fitting of circles and ellipses," in BIT, vol. 34, 1994, pp. 558–875.

[12] J. Vandorpe, H. V. Brussel, and H. Xul, "Exact dynamic map building for a mobile robot using geometrical primitives produced by a 2d range finder," in in Robotics and Automation, 1996. Proceedings., 1996 IEEE International Conference on, vol. 1, 1996, pp. 901–908.

[13] Z. Shiller, O. Gal, and T. Fraichard, "The nonlinear velocity obstacle revisited: the optimal time horizon," in Workshop on Guaranteeing Safe Navigation in Dynamic Environments, the 2010 IEEE Int. Conf. on Robotics and Automation, Anchorage, AK (US), 2010.

[14] K. J. Lee, "Reactive navigation for an outdoor autonomous," in in Mechanical and Mechatroinc Engineering vol. Master: University of Sydney, 2001.

[15] [K. Dietmayer, J. Sparbert, and D. Streller, "Model based object classification and object tracking in traffic scenes from range images," in In Proceedings of intelligent Vehicles Symposium, 2001.

[16] S. Santos, F. S. J.E. Faria and, R. Araujo, and U. Nunes, "Tracking of multi-obstacles with laser range data for autonomous vehicles," in in 3rd National Festival of Robotics Scientific Meeting (ROBOTICA) Lisbon, Portugal, 2003, pp. 59–65.

[17] K. Rebai, A. Benabderrahmane, O. Azouaoui, and N. Ouadah, "Moving obstacles detection and tracking with laser range finder," in in Advanced Robotics, 2009. ICAR 2009. International Conference onl, 2009, pp. 1– 6.

[18] H. Koshimizu, K. Murakami, M. Numada, Global feature extraction us- ing ecient hough transform, in: in Industrial Applications of Machine Intelligence and Vision, 1989, pp. 298303.

[19] D. Dagao, M. Q. X. Meng, H. Zhongming, W. Yueliang, An improved hough transform for line detection, in: in Computer Application and System Mod- eling (ICCASM), 2010 International Conference on, 2010, pp. 354357.

[20] K. O. A. a. R. Y. Siegwart, Feature extraction and scene interpretation for map-based navigation and map building, in: in Proc. of SPIE, Mobile Robotics XII, 1997.

[21] V. Nguyen, A. Martinelli, N. Tomatis, R. Siegwart, A comparison of line extraction algorithms using 2d laser rangender for indoor mobile robotics, in: in Intelligent Robots and Systems, 2005. (IROS 2005). 2005 IEEE/RSJ International Conference on, 2005, pp. 19291934.

[22] A. S. a. A. K. a. S. K. a. M. D. a. R. HUSSON, An optimized segmentation method for a 2d laser-scanner applied to mobile robot navigation, in: in In Proceedings of the 3rd IFAC Symposium on Intelligent Components and Instruments for Control Applications, 1997.

[23] M. M. Romera, M. A. S. VÃa¸zquez, and J. C. G. GarcÃ a, "Tracking multiple and dynamic objects with an extended particle filter and an adapted k-means clustering algorithm," in Preprints of the 5th IFAC/EURON